Hydrogeology and Deformation of Sandbars in Response to Fluctuations in Flow of the Colorado River in the Grand Canyon, Arizona

U.S. GEOLOGICAL SURVEY
Water-Resources Investigations Report 95—4010

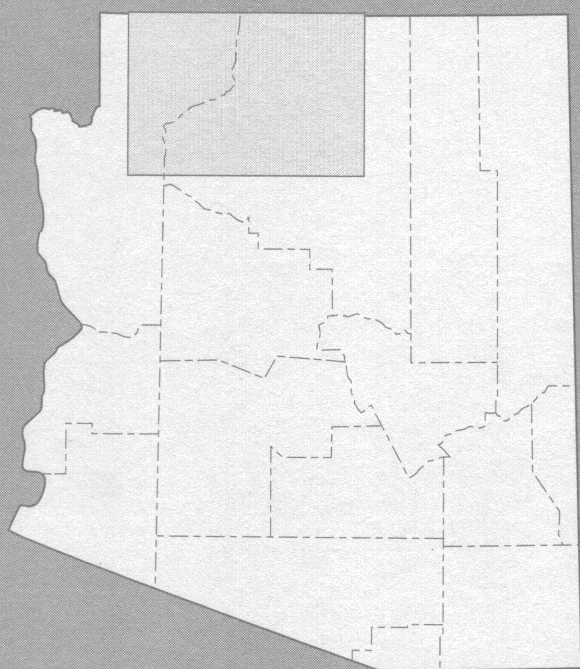

Prepared in cooperation with the
BUREAU OF RECLAMATION

Hydrogeology and Deformation of Sandbars in Response to Fluctuations in Flow of the Colorado River in the Grand Canyon, Arizona

By MICHAEL C. CARPENTER, ROBERT L. CARRUTH, JAMES B. FINK, JAMES K. BOLING, and BRIAN L. CLUER

U.S. GEOLOGICAL SURVEY
Water-Resources Investigations Report 95—4010

Prepared in cooperation with the
BUREAU OF RECLAMATION

Tucson, Arizona
1995

U.S. DEPARTMENT OF THE INTERIOR
BRUCE BABBITT, Secretary

U.S. GEOLOGICAL SURVEY
Gordon P. Eaton, Director

For additional information write to:

District Chief
U.S. Geological Survey
Water Resources Division
375 South Euclid Avenue
Tucson, AZ 85719-6644

Copies of this report can be purchased from:

U.S. Geological Survey
Open-File Section
Box 25286, MS 517
Denver Federal Center
Denver, CO 80225

CONTENTS

Page

Abstract 1
Introduction 1
  Methods and quality control 2
Hydrogeology and deformation 4
  Sandbar –6.5R 4
  Sandbar 43.1L 4
  Sandbar 172.3L 11
Effects of flow on sandbar deformation 12
Summary and conclusions 13
Selected references 16

FIGURES

1. Map showing location of sandbars –6.5R, 43.1L, and 172.3 L 2
2. Diagram showing geologic section and location of sensors at sandbar –6.5R, upstream from Lees Ferry 4
3. Diagram showing geologic section and location of sensors at sandbar 43.1L, opposite Anasazi Bridge 5
4. Diagram showing modified logarithmic pseudosection of apparent resistivity referenced to land surface at sandbar 43.1L, opposite Anasazi Bridge, August 1991 6
5. Graph showing block-averaged, apparent resistivity from sandbar 43.1L, opposite Anasazi Bridge, in relation to theoretical half-space depth of investigation 7
6. Graph showing tilt for sensor I18 at sandbar 43.1L, opposite Anasazi Bridge, April 8 through August 31, 1991 8
7. Graph showing river stage at sandbar 43.1L, opposite Anasazi Bridge, April 8 through June 21, 1991 8
8. Graph showing water level in piezometer 46 at sandbar 43.1L, opposite Anasazi Bridge, April 8 through August 31, 1991 9
9. Graph showing water level in piezometer 40 at sandbar 43.1L, opposite Anasazi Bridge, April 8 through August 31, 1991 9
10. Graph showing water level in piezometer 37 at sandbar 43.1L, opposite Anasazi Bridge, April 8 through August 31, 1991 10
11. Graph showing water level in piezometer 42 at sandbar 43.1L, opposite Anasazi Bridge, April 8 through August 31, 1991 10
12. Diagram showing geologic section and location of sensors at sandbar 172.3L, downstream from the mouth of National Canyon 12
13. Diagram showing modified logarithmic pseudosection of apparent resistivity referenced to land surface at sandbar 172.3L, downstream from the mouth of the National Canyon, August 1991 13
14. Graph showing tilt for sensors I11, I41, and I47 at sandbar 172.3L, downstream from the mouth of National Canyon, April 19 through September 12, 1991 14
15. Graph showing river stage at sandbar 172.3L, downstream from the mouth of National Canyon, April 19 through September 12, 1991 14

CONTENTS

FIGURES—Continued

	Page
16. Graph showing water level in piezometer 56 at sandbar 172.3L, downstream from the mouth of National Canyon, April 19 through September 12, 1991	14
17. Graph showing water level in piezometer 64 at sandbar 172.3L, downstream from the mouth of National Canyon, April 19 through September 12, 1991	15

TABLE

1. Results of one-dimensional modeling of the central part of sandbar 43.1L 7

CONVERSION FACTORS

Multiply	By	To obtain
millimeter (mm)	0.03937	inch
meter (m)	3.281	foot
cubic meter per second (m^3/s)	35.31	cubic foot per second
kilopascal (kPa)	0.1450	pound per square inch

Temperatures are given in degrees Celsius (°C), which can be converted to degrees Fahrenheit (°F) by the following equation:

$$°F = 1.8(°C) + 32$$

Specific conductance is given in microsiemens per centimeter (µS/cm) at 25 degrees Celsius.

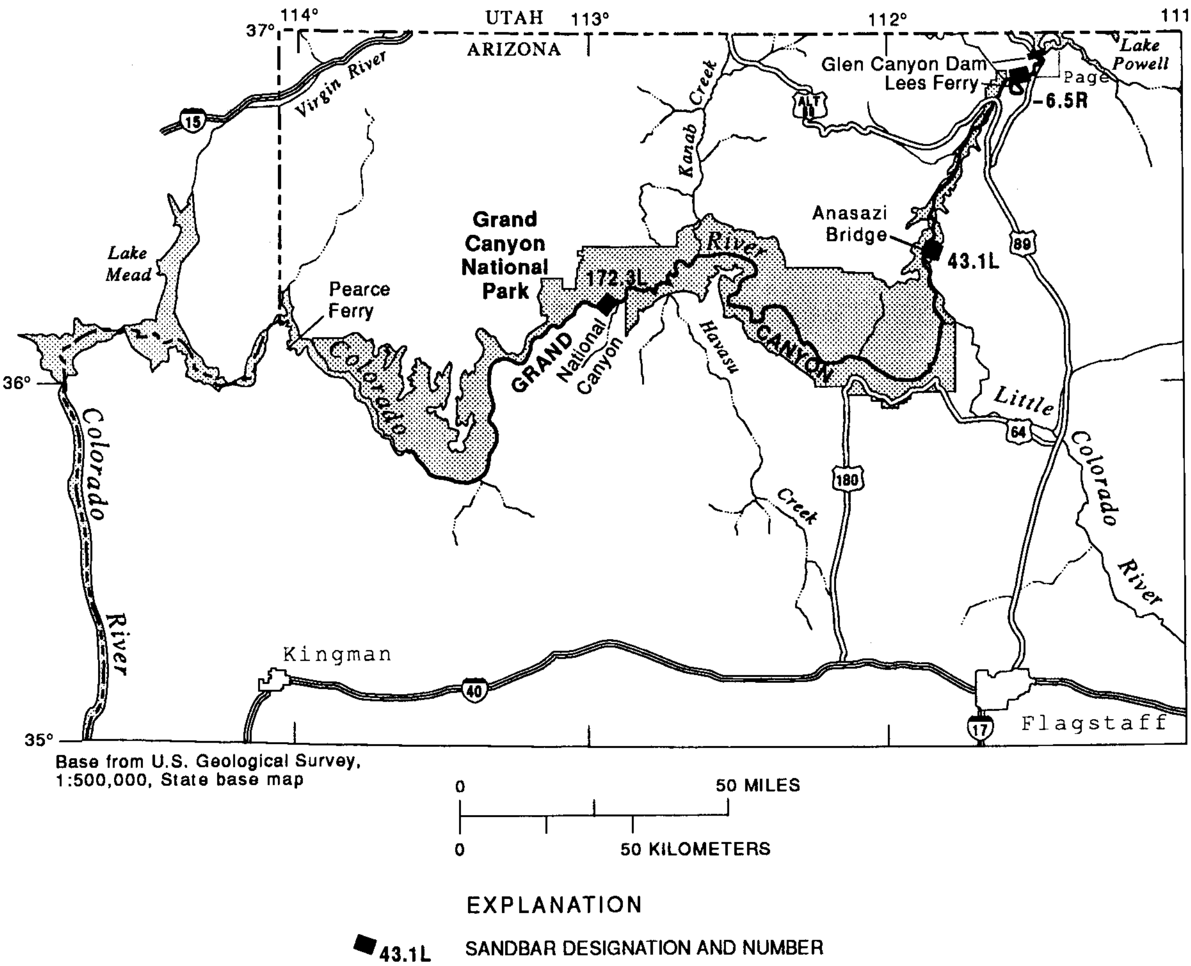

Figure 1. Location of sandbars −6.5R, 43.1L, and 172.3 L.

Methods and Quality Control

Three sandbars were instrumented with sensors for continual monitoring of stage, pore pressure, temperature, and tilt to determine the relation between ground-water flow and sandbar deformation. The instrumentation plan at each sandbar included deep, intermediate, and shallow pairs of pore-pressure and temperature sensors arrayed in a vertical plane orthogonal to the river's edge. The clusters were spaced a few meters apart in the zone of fluctuating river stage to determine the vertical component of ground-water flow in the deforming sandbar face. The clusters were spaced more than 10 m apart in the middle and back of the sandbar. Seven tilt sensors were arrayed both parallel with and orthogonal to the river's edge in the deforming sandbar face. Two vertical clusters of tensiometers at three depths were also set in the sandbar. A pressure-sensor, temperature-sensor pair was installed at the sand-water interface below the zone of fluctuating river stage to function as a stage sensor.

Variations from the instrumentation plan existed at each sandbar. Sandbar −6.5R had no tilt sensors and no tensiometers. At sandbar 43.1L, tensiometers were in vegetated and unvegetated soil. At sandbar 172.3L, tensiometers were in a medium sand and a lower bench of silty, very fine sand.

Piezometers were placed in the sandbars using a jetting and driving technique. Water was pumped

Hydrogeology and Deformation of Sandbars in Response to Fluctuations in Flow of the Colorado River in the Grand Canyon, Arizona

By Michael C. Carpenter, Robert L. Carruth, James B. Fink, James K. Boling, *and* Brian L. Cluer

Abstract

Rill erosion, slumping, and fissuring develop on seepage faces of many sandbars along the Colorado River in the Grand Canyon. These processes, observed at low river stage, are a response to residual head gradients in the sandbars caused by the river-stage fluctuation. Three sandbars were instrumented with sensors for continual monitoring of pore pressure and ground-water temperature within the sandbars and river stage. Two of the sandbars also had tilt sensors to aid in determining the relation between ground-water flow within and out of the sandbars and sandbar deformation. Tilting at sandbar 43.1L occurred on the downward limb of the hydrograph in the absence of scour, indicating slumping or a slump-creep sequence. The deformation was caused by outward-flowing bank storage, oversteepening of the lower part of the slope in the zone of fluctuating river stage by rilling, and increased effective stress. At sandbar 172.3L, tilts were probably all related to scour and occurred on the rising limb of a hydrograph. Tilt occurred on April 17, May 7, May 13, June 18, and September 1, 1991. On September 1, the entire face of sandbar 172.3L was scoured. Rill erosion and slumping accompanied by measured tilts continued in reduced magnitude on sandbar 43.1L during interim flows. Thus, reduction in the range of discharge does not eliminate degradation caused by rill erosion, slumping, and fissuring. The importance of the ground-water processes is that they occur on every sandbar and become increasingly important on all sandbars in the absence of sandbar-building flows.

INTRODUCTION

Discharge from Glen Canyon Dam on the Colorado River can fluctuate from less than 85 to more than 850 m^3/s on a daily basis. Corresponding stage fluctuations on downstream sandbars can exceed 3.4 m. Rill erosion, slumping, and fissuring on seepage faces of many sandbars, observed at low river stage, are a response to residual head gradients in the sandbars caused by the river-stage fluctuation. Seepage faces probably develop on all sandbars in the study area.

The study was designed to document the processes of seepage erosion, slumping, and fissuring and to establish relations among material properties of sandbar sediments, threshold of hydraulic gradient for rill erosion, and effective stresses causing slumping. During the study, three sandbars were instrumented (fig. 1), and data were collected for intended studies of variably saturated ground-water flow, deformation, and heat flow. This report provides preliminary findings of data from the three sandbars. The report describes the stratigraphy of the three sandbars, the hydrogeology and tilt events on the two downstream sandbars, and the effects of flow on sandbar deformation.

HYDROGEOLOGY AND DEFORMATION

Sandbar –6.5R

Sandbar –6.5R[1] (fig. 2), upstream from Lees Ferry, consisted of a unit of homogeneous fine to medium sand underlain by a confining unit of silty, very fine sand. The confining unit was 0.14 m thick where it cropped out in a gully that was eroded into the sandbar in the fall of 1991. The unit dipped toward the back of the sandbar where it flattened and attained a depth of about 3.5 m. The confining unit was underlain by another unit of fine to medium sand. The back boundary of the sandbar was sloping talus and there was no return channel. This sandbar had a gentle slope in the zone of fluctuating river stage and exhibited a seepage face with rill erosion but did not exhibit slumping and fissuring. This sandbar was considered to be a control for comparison with the two deforming sandbars. Tilt sensors were not installed in sandbar –6.5R; therefore, this sandbar is not discussed further in this report.

[1]Sandbar names in this report reflect their locations according to the customary distance downstream from Lees Ferry.

Sandbar 43.1L

Sandbar 43.1L (fig. 3) consisted of homogeneous fine to medium sand overlying medium salt-and-pepper sand at a depth of 6 m. The back boundary was talus with a narrow, deep return channel underlain by a thin, clayey silty sand. A

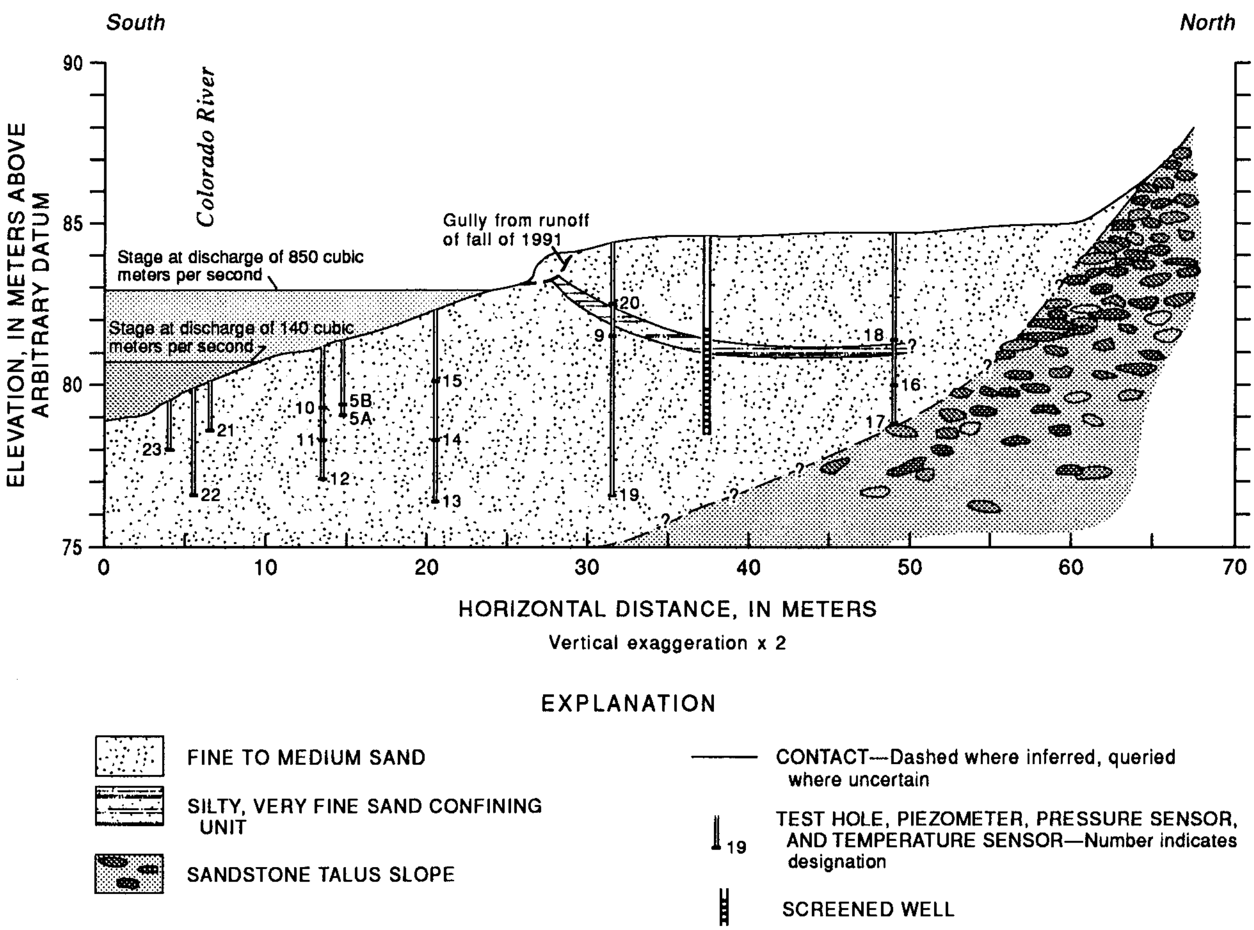

Figure 2. Geologic section and location of sensors at sandbar –6.5R, upstream from Lees Ferry.

from the river down a 13-millimeter-diameter polyvinyl chloride (PVC) pipe for jetting inside and near the bottom of 50-millimeter-diameter PVC flush-thread pipe used for temporary casing. A 1-meter section of flush-thread pipe was fitted with a coupling on the outside near the bottom to make a driver. A fence-post-type hammer with a hole in the top to fit over the pipe but not over the coupling was used to drive the string of flush-thread pipe by hammering on the coupling with the 1-meter section as the top section of the string. Maximum depth reached was 10 m. The pressure sensor was a Motorola MPX2200AS 0 to 200 kPa absolute device. The sensor was attached to the tip of a 13-millimeter PVC pipe that was fitted with a fine nylon screen about 75 mm long and lowered into the 50-millimeter casing. The casing was then pulled from around the piezometer. In vertical nests of piezometers, each piezometer was set in its own drilled hole. This eliminated the possibility of pressure contamination from lower in the drill hole. Because the pressure sensors were absolute devices, additional pressure sensors were used as barometers to remove the effect of atmospheric-pressure fluctuations. Because of the importance of the pressure correction, each site had three barometers for redundancy. Resolution of the pressure sensors in the datalogging system was 3 mm of water-level fluctuation. The temperature sensors were Campbell Scientific 107B thermistors that were inserted to the bottom of the 13-millimeter PVC pipes adjacent to the pressure sensors. Resolution of the temperature sensors is less than 0.01°C, but specified accuracy is ±0.2°C. Observed performance was ±0.5°C before correction for field-calibration checks. Data were recorded on Campbell Scientific CR10 dataloggers with multiplexers and storage modules. Excitation voltage to pressure sensors was provided by switched regulated circuits with a voltage stability of ±0.01 percent. The electronic equipment was buried in a sealed, metal box containing desiccant.

The pressure sensors were calibrated at three temperatures and five pressures in a Dewar flask in an isothermal bath. Pressure sensors were calibrated and field checked using a Paroscientific model 760 Portable Pressure Standard with a range of 0 to 690 kPa absolute and an accuracy of ±0.01 percent. The primary temperature standard was a certified Ever Ready thermometer with an accuracy of ±0.03°C. The secondary standard for field use was a Doric digital thermometer for a YSI 401 thermistor. Accuracy of the secondary standard against the primary standard was ±0.1°C. The tilt sensors were calibrated using an accurately cut 10° angle for three-point calibration at +10°, 0°, and -10° from an arbitrary near-horizontal plane. In the field, temperature sensors were placed with all pressure sensors and most tilt sensors. Pressure sensors used for water levels were field checked by measuring depth to water in the 13-millimeter pipes for all sensors that were accessible at the time of a site visit. Submerged pressure sensors, including stage sensors, were checked using surveyed river stage at known times. Accessible temperature sensors were checked by pulling them out of the 13-millimeter pipes and putting the sensors in a thermos bottle with the secondary standard at two temperatures.

In conjunction with the long-term ground-water monitoring efforts, high-resolution, DC resistivity studies were performed at sandbars 43.1L and 172.3L during August 1991. DC resistivity offered the potential for detecting vertical and lateral differences in the electrical properties of the sandbars. The differences in electrical properties are related to moisture content, porosity, and relative clay content of the sandbars. All of these properties are of interest regarding the hydraulic behavior of the sandbars.

A pole-pole electrode array was used that allowed maximum depth of investigation and also allowed small interelectrode spacings for good lateral resolution. Interelectrode spacings ranged from 1.5 to 38 m. Infinite (remote) electrodes were placed upstream and downstream from the survey lines at distances greater than 10 times the maximum interelectrode spacing. Time constraints allowed only one line perpendicular to the sandbar from the cliff wall to the river's edge.

The data are presented in modified pseudosections that are referenced to the land surface. The location of the plot points in the modified pseudosections are determined by a logarithmic transformation developed by Fink (1989). Referencing the pseudosection to the land surface lends a more geologic appearance to the data but does not alter the fact that the plots are still pseudosections.

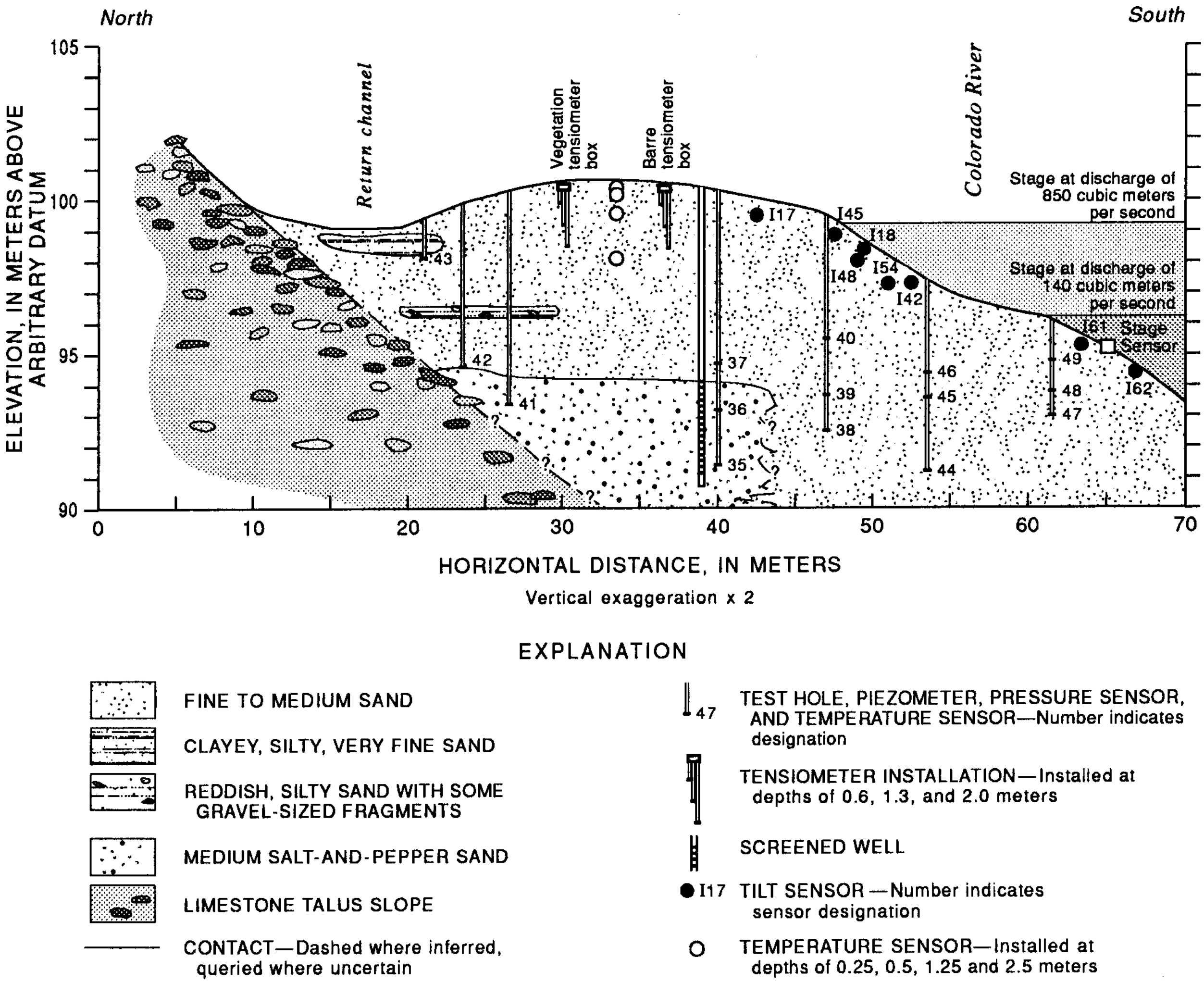

Figure 3. Geologic section and location of sensors at sandbar 43.1L, opposite Anasazi Bridge.

second reddish, silty sand with some gravel occurred at a depth of about 4 m in the back of the sandbar. The zone of fluctuating river stage was a steeply sloping face that exhibited rill erosion, slumping, and fissuring.

A single line of pole-pole DC resistivity was performed at sandbar 43.1L. The line was 36.5 m long and crossed the sandbar transversely, north to south, beginning at the base of the canyon wall next to outcrop and continuing across the elevated, dry-sand part of the sandbar, and down the sandbar face into the Colorado River approximately 1.5 m (fig. 4). The first 5 m of the line was in a return channel adjacent to the cliff base.

Apparent resistivities ranged from 50 to more than 2,000 ohm-meters (Ω-m). The high apparent resistivities were related to the dry-sand part of the sandbar that underlay approximately 18 m of the line. Data from the central part of the line were block-averaged and modeled using one-dimensional methods. Modeling results indicated that the dry sand had a true resistivity of about 3,800 Ω-m and a thickness of about 1.6 m (fig. 5, table 1). This thickness correlated well with the elevation of the dry-sand part of the sandbar above the average stage of the river during the measurement period. Low apparent resistivities occurred on both ends of the line where electrodes were either occasionally submerged in the river or in the return channel. Apparent resistivities in these areas ranged from 40 to 50 Ω-m, suggesting that the river-water resistivity was not any greater than

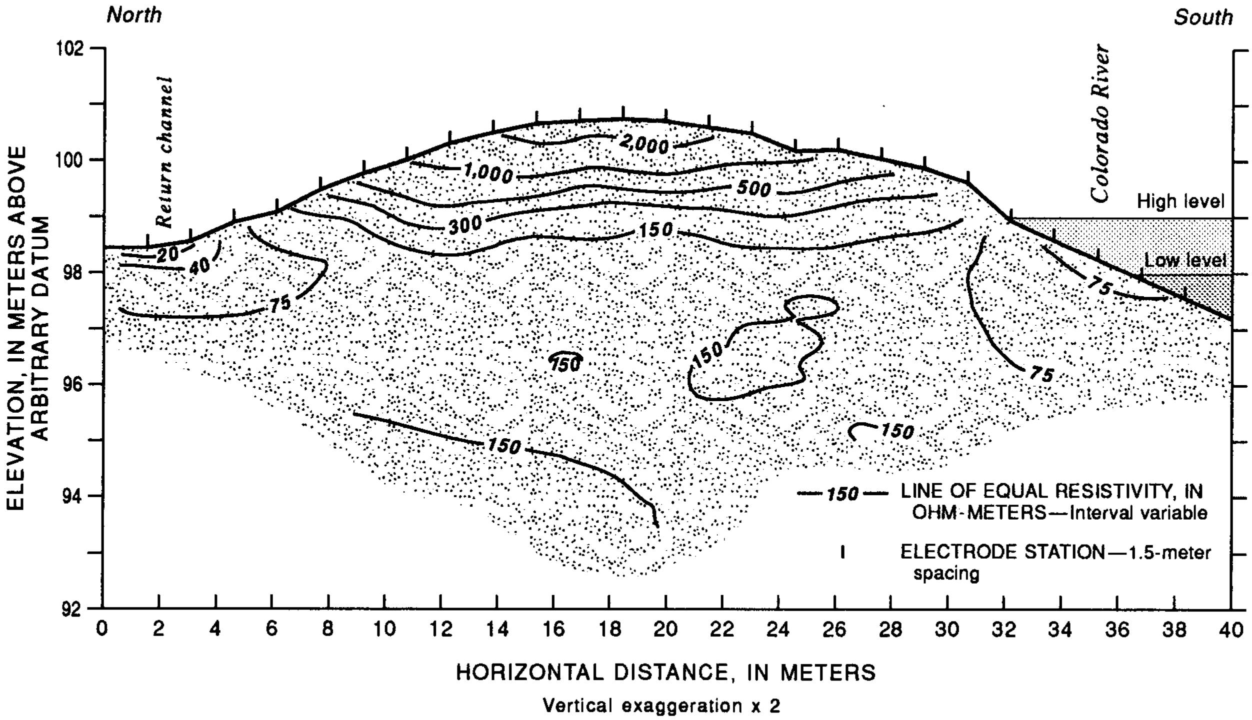

Figure 4. Modified logarithmic pseudosection of apparent resistivity referenced to land surface at sandbar 43.1L, opposite Anasazi Bridge, August 1991.

50 Ω-m. (A resistivity of 50 Ω-m is equivalent to an electrical conductivity of 200 μS/cm.) Resistivity values of about 40 Ω-m occurred in the return channel. These resistivity values probably were lower than the river water because of the clay content in the sediments underlying the return channel or greater dissolved solids in the stagnant return-channel water.

The low apparent near-surface resistivities at the ends of the line also were reflected in the middle layer, for which modeling suggested a true resistivity of 50±20 Ω-m and a thickness of 8.5±4.0 m. The middle layer was inferred to represent saturated sand and the overlying capillary zone.

Modeling yielded a higher true resistivity for the third layer that may represent electrical bedrock. The maximum depth penetrated by any of the piezometers was approximately 10 m. Bedrock was not encountered nor was there any significant change observed in grain size that might indicate penetration of a basal gravel or talus. On the basis of the resistivity data, bedrock may have been just below the limit of drilling at an estimated depth of 10 to 15 m.

Tilt is a change in inclination of a zone or a shear strain in a vertical plane. The sign and axis conventions used in this report are: the positive x axis is orthogonal to and points toward the river, and tilt of the x axis is positive when the sensor rotates counterclockwise when viewed from upstream on the left bank; the positive y axis is parallel with the river and points downstream, and tilt of the y axis is positive when the sensor rotates counterclockwise when viewed from the river looking toward the sandbar on the left bank. Positive tilt may also be thought of as upward and negative tilt as downward when viewed along the axis. In a medium that can be treated as two-dimensional (reflecting plane strain), all deformation will occur in the plane defined by the x axis and the vertical (or z) axis, that is, orthogonal to the river. A sensor within a slump block or rotational failure will exhibit positive x tilt. A sensor within a zone undergoing creep or within a zone on the riverward side of a fissure during early

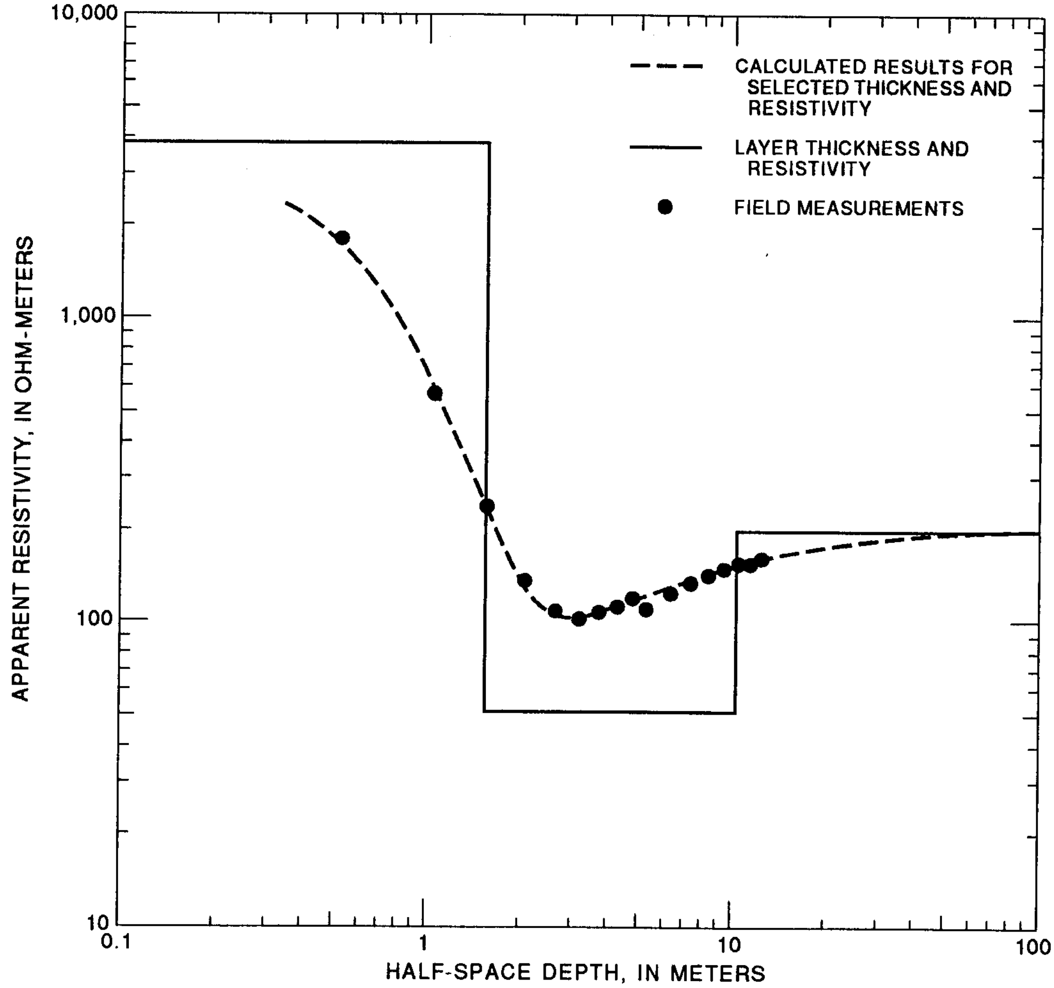

Figure 5. Block-averaged, apparent resistivity from sandbar 43.1L, opposite Anasazi Bridge, in relation to theoretical half-space depth of investigation.

Table 1. Results of one-dimensional modeling of the central part of sandbar 43.1L

[Ω-m, ohm-meters; m, meters; NA, not applicable]

Layer	Resistivity (Ω-m)	Range (Ω-m)	Thickness (m)	Range (m)
1	3,800	±400	1.6	±0.10
2	50	±20	8.5	±4.0
3	200	±25	Infinite	NA

stages of a process similar to glacial calving will exhibit negative x tilt.

At sandbar 43.1L, a sequence of tilts occurred from July 7, 1991, through July 17, 1991 (fig. 6). The tilts were at least five times greater in the x tilt sensor, which is oriented orthogonal to the river, than in the y tilt sensor, which is oriented parallel to the river. The major tilts were preceded by tilt of –0.1° toward the river (along the x axis) on the morning of July 2, and tilt of 0.1° toward the river on the evening of July 6. At 8:00 a.m. on July 7, tilt of 5.5° occurred toward the river. At 9:00 a.m. on July 12, tilt of –0.5° occurred; and at 9:00 a.m. on July 17, an additional tilt of –3.3° occurred. These major tilts were followed by continued negative tilt in the x sensor from July 18 to July 26, punctuated with daily spikes of about –0.4° that occurred in the morning. With the single exception of the precursor positive tilt on July 6, all of the sudden tilts occurred on downward limbs of the hydrographs (figs. 7–11)

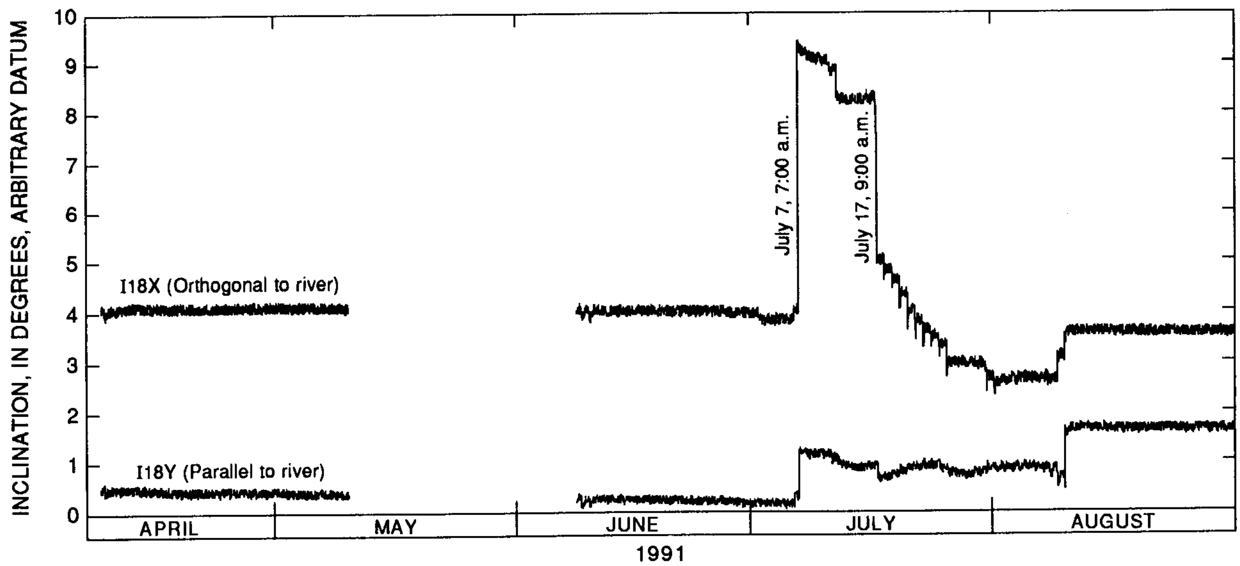

Figure 6. Tilt for sensor I18 at sandbar 43.1L, opposite Anasazi Bridge, April 8 through August 31, 1991.

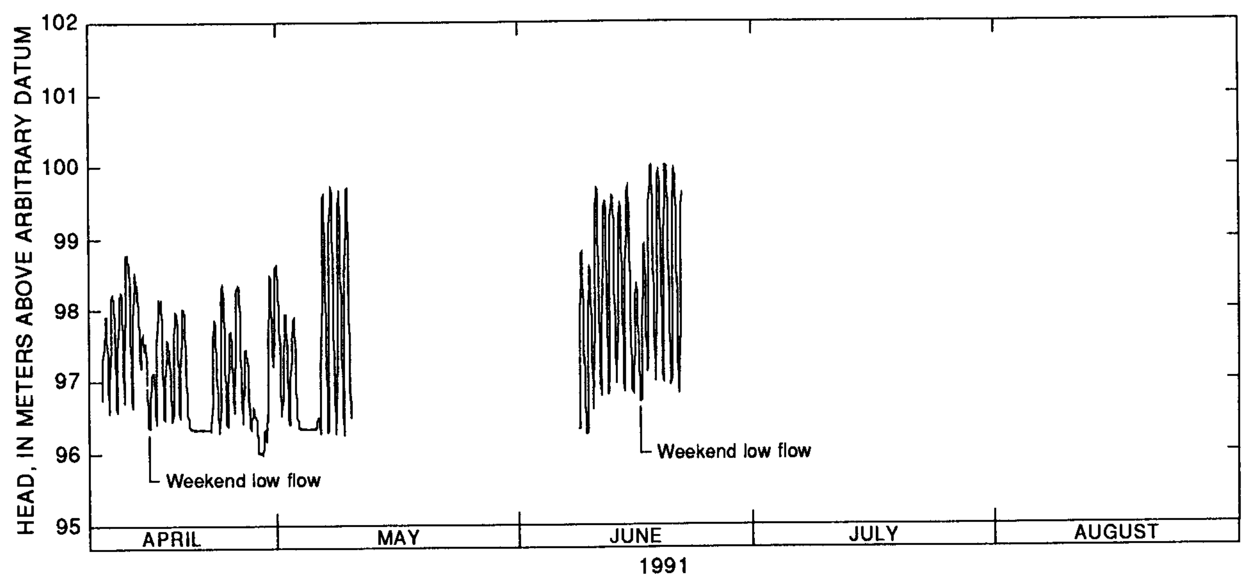

Figure 7. River stage at sandbar 43.1L, opposite Anasazi Bridge, April 8 through June 21, 1991.

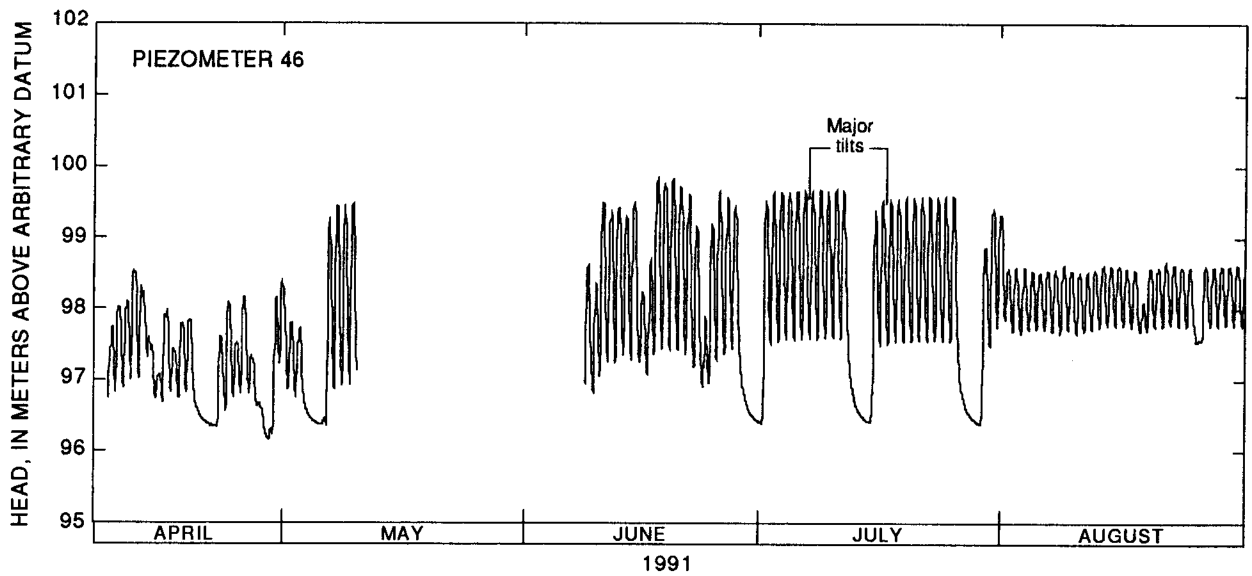

Figure 8. Water level in piezometer 46 at sandbar 43.1L, opposite Anasazi Bridge, April 8 through August 31, 1991.

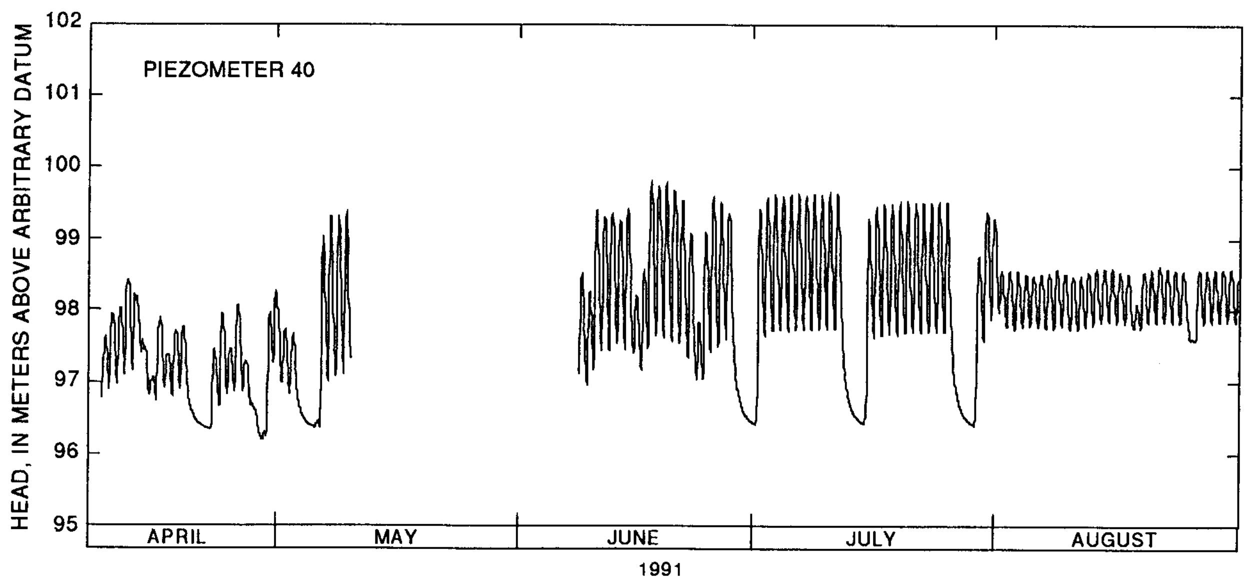

Figure 9. Water level in piezometer 40 at sandbar 43.1L, opposite Anasazi Bridge, April 8 through August 31, 1991.

when the effective stress (intergranular stress) in the sandbar face was increasing. The hypothesis suggested by this sequence of tilts is slumping or rotational failure, in which tilt sensor I18 was within a slump block during the major upward tilt on July 7, followed by several occurrences of creep. An alternative hypothesis is slumping with tilt sensor I18 within the slump block on July 7 followed by slumping with tilt sensor I18 outside the slump block on subsequent tilts. The sensor may have had a tendency to realign itself in a preferred orientation or may have been affected by the cable connecting the sensor to the datalogger, in spite of efforts to prevent such problems. The slope failure was shallow because none of the nearby tilt sensors—I17, I45, I48, or I54—(fig. 3) exhibited any tilt during April to July 1991. Tilt sensor I42 failed in April 1991. The probable cause of slope

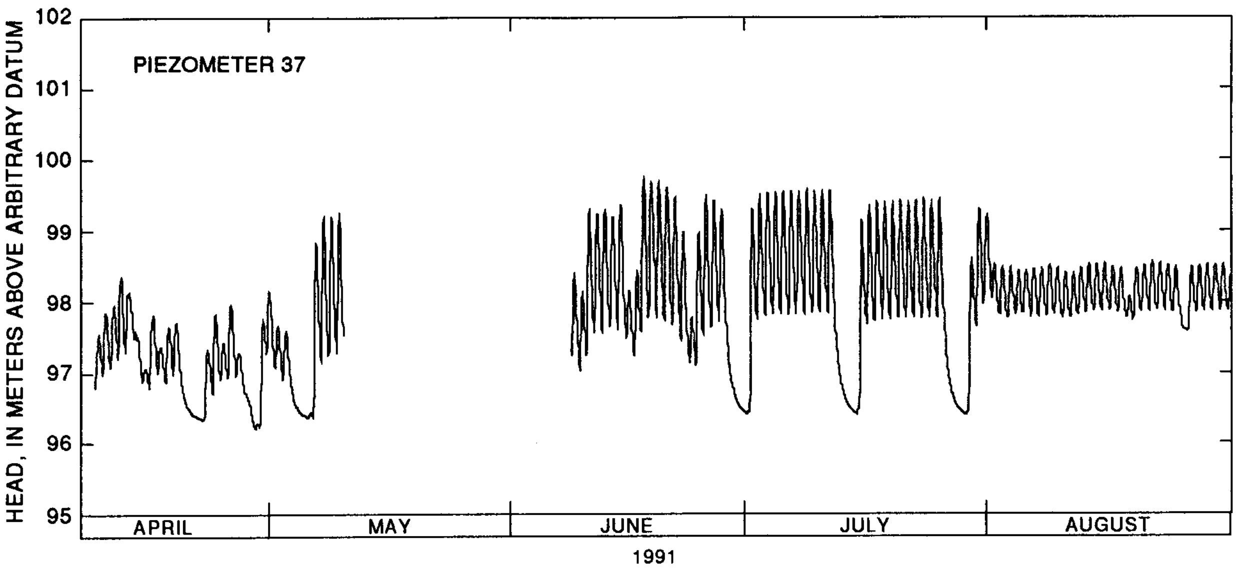

Figure 10. Water level in piezometer 37 at sandbar 43.1L, opposite Anasazi Bridge, April 8 through August 31, 1991.

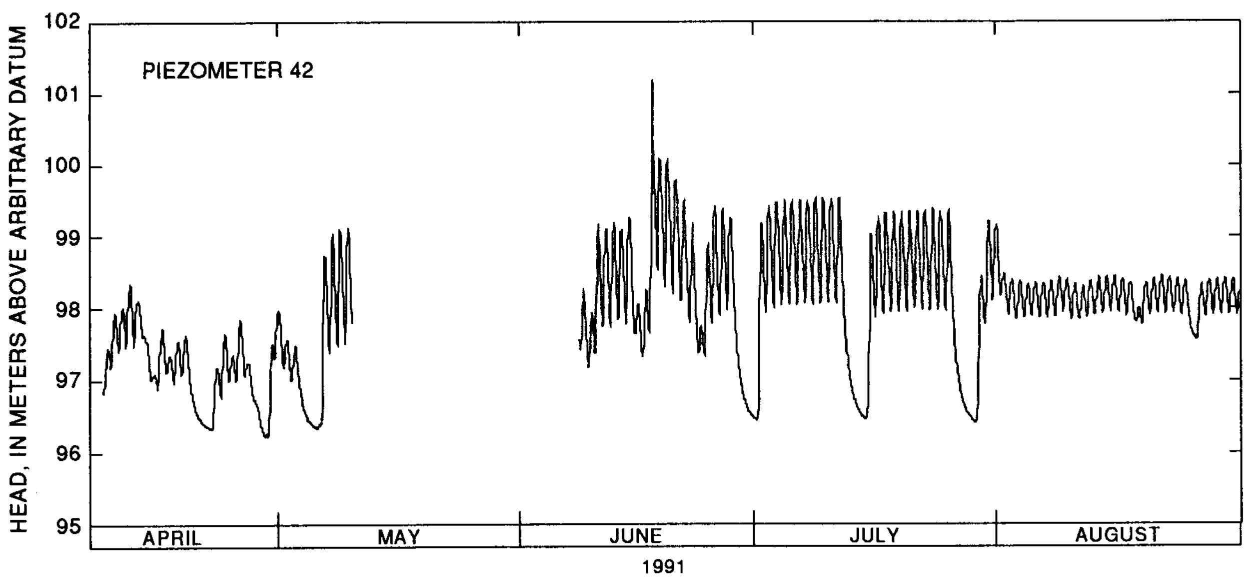

Figure 11. Water level in piezometer 42 at sandbar 43.1L, opposite Anasazi Bridge, April 8 through August 31, 1991.

failure on this sandbar was oversteepening of the lower part of the slope in the zone of fluctuating river stage. This conclusion was supported by evidence of rill erosion in daily photographs taken automatically from the opposite bank (Cluer, 1991). Rilling was enhanced during fluctuating weekend low flows (fig. 7). Rilling was intense after about 1.5 days during research steady low flows.

Attenuation of water-level fluctuation from the front to the back of sandbar 43.1L was evident at piezometers 46, 40, 37, and 42 (figs. 9–11). From piezometer 46 to piezometer 42, the attenuation of fluctuating July flows was 30 percent over a distance of 30 m. The particularly high water level in piezometer 42 beginning on June 17, 1991, (fig. 11) may have been caused by hydraulic

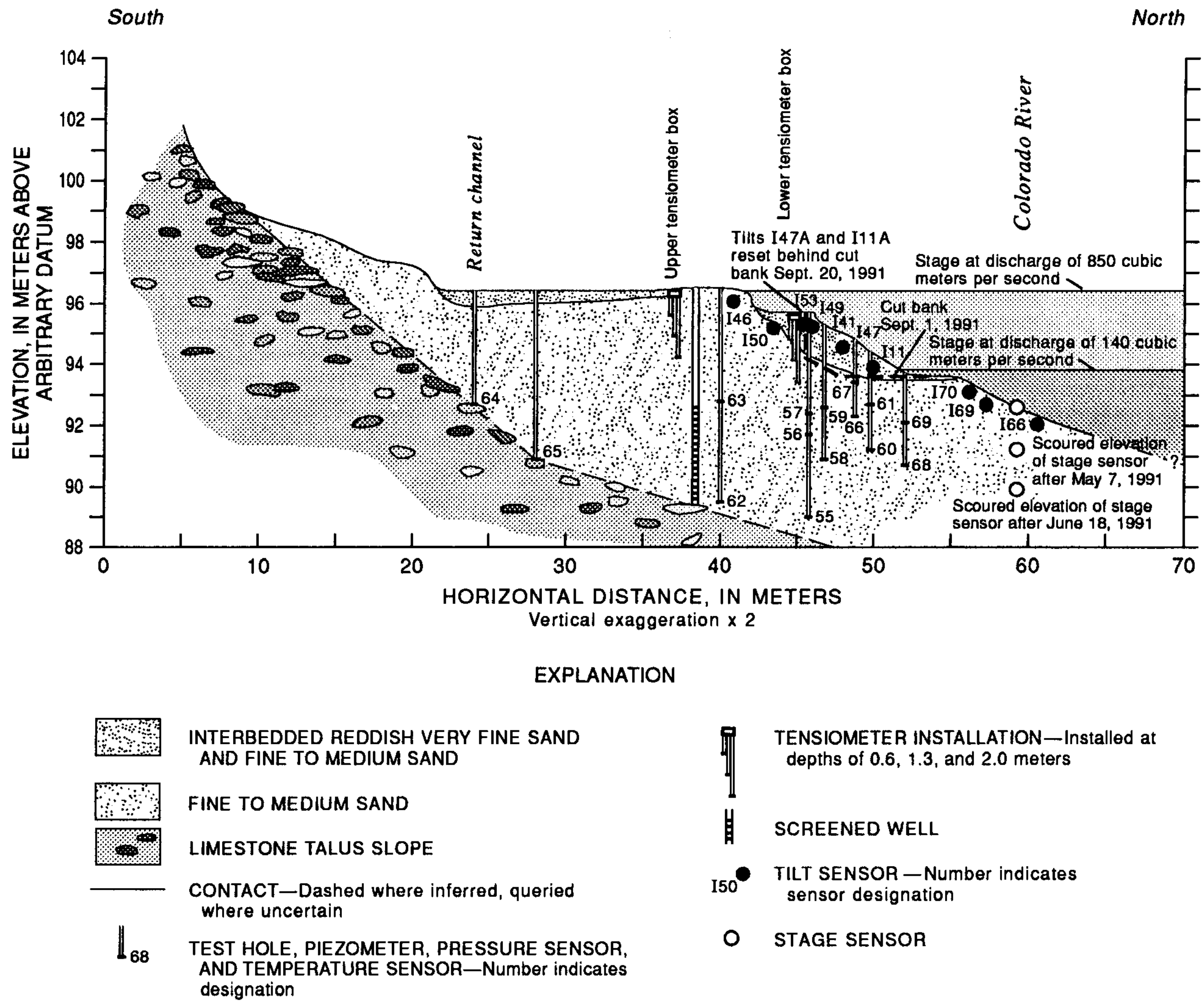

Figure 12. Geologic section and location of sensors at sandbar 172.3L, downstream from the mouth of National Canyon.

at ±12° about 5:00 p.m., followed by sensors I41 and I47 at 7:00 p.m.

At sandbar 172.3L, attenuation of water-level fluctuation was about 30 percent from the stage sensor to piezometer 56 and 65 percent from the stage sensor to piezometer 64 over a distance of 35 m (figs. 15–17). Water-level fluctuations were less attenuated at piezometer 56 after the June 18, 1991, scour that deepened the stage sensor. The stage sensor was scoured and buried successively 1.3 m and 1.8 m on May 7 and June 18, 1991. The change in attenuation from the stage sensor to piezometer 56 probably was caused by the combination of scour removing low-permeability material near piezometer 56 and burial reducing water-level fluctuations at the stage sensor.

EFFECTS OF FLOW ON SANDBAR DEFORMATION

At this stage of analysis, only qualitative statements can be made regarding effects of fluctuating flow on bank-storage processes and the flow alternatives. Daily photographs of sandbar 43.1L, taken automatically in June and July of 1991 connection to an upstream part of the return channel or overpressurization by a process such as temporary sealing of a zone accompanied by swelling of clays. Piezometer 42 exhibited no evidence for movement or failure throughout its record.

Sandbar 172.3L

Sandbar 172.3L (fig. 12) consisted of interlayered fine to medium sand and silty, very fine sand. The back boundary was talus abutted by a broad shallow return channel underlain by silty fine sand. The zone of fluctuating river stage was a steeply sloping face with a bench that was underlain by reddish, silty, very fine sand interlayered with fine to medium sand. This sandbar exhibited rill erosion, slumping, and fissuring.

A single line of pole-pole DC resistivity was performed at sandbar 172.3L. The line was 38 m long and crossed the sandbar transversely, south to north, beginning at the base of the talus slope and continuing across the elevated, dry-sand part of the sandbar down the sandbar face into the Colorado River (fig. 13). The first 9 m of the line was in an elevated, dry-sand part of the sandbar. The central part of the line crossed a silty, very fine sand bench for approximately 17 m before dropping off the sandbar face. The north end of the line terminated 3 m into the river. The topography of this survey line was more irregular than the line at sandbar 43.1L and resulted in greater localized variations in the observed apparent resistivities. Well-defined layered-earth responses were not evident in the data, and one-dimensional modeling was not applied.

Apparent resistivities ranged from 25 Ω-m to greater than 1,000 Ω-m. The highest values were associated with dry sand at the south end of the line and near the top of the sandbar. Although the central part of the line was well vegetated and had a higher percentage of silt and clay, the associated apparent resistivities were greater than 100 Ω-m. A decrease in apparent resistivity with increasing spacing in the central part of the line suggested a more conductive lower horizon, but effects caused by surface topography or perhaps lateral changes in porosity or permeability masked the deeper effects. Drilling encountered obstacles at depths ranging from 4 to 7 m. If bedrock had been present at these shallow depths, a significant increase in apparent resistivity should have occurred at wider electrode spacings. A generally decreasing trend as a function of increasing spacing suggested that bedrock was not detected and that the obstacles encountered during drilling were probably talus blocks rather than in-place bedrock. Depth to bedrock appeared to be greater than 20 m.

The two most salient features in the apparent resistivity pseudosection were the two lows associated with sharp changes in topography. The low near the return channel was likely restricted to changes in topography. The low beneath the bench on the sandbar face appeared to be related to a combination of changes in topography and subsurface lithology. The inferred subsurface change may have been caused by a facies change or a zone of increased porosity.

Several tilts occurred at sandbar 172.3L. At this sandbar, the tilts documented by tilt sensors occurred on the rising limb of a hydrograph and probably were all related to scour. Major scour accompanied by tilt began about 11:00 p.m. April 17 and lasted until about 1:30 a.m. April 18, 1991. This scour was observed by the crew installing the sensors before sensors were operational in the sandbar. In this scour event, which also occurred on the rising limb of the hydrograph, a large sand peninsula in the upstream end of the eddy was completely eroded. Scour events documented by tilt sensors and daily photographs taken automatically by a camera on the opposite bank include May 7, 1991, at about 7:30 p.m.; May 13, 1991; June 18, 1991, about 7:30 p.m.; and September 1, 1991. Minor tilting of –0.3° in both axes of tilt sensor I41 occurred in the 2 days following the May 7 tilt (fig. 14). No other tilt sensors exhibited any tilt during this period.

On June 18, tilt sensor I11 went off scale at ±12° about 8:00 p.m. Sensors I41 and I47 tilted about 9:00 a.m. on June 19. Sensor I41 tilted –1.1° in the x-axis and –0.7° in the y-axis in the 5 days following June 18. The succession of tilts from sensors in the river to sensors farther into the sandbar indicated failure by scour. On September 1, 1991, the entire face of sandbar 172.3L was scoured. Tilt sensor I11 went off scale

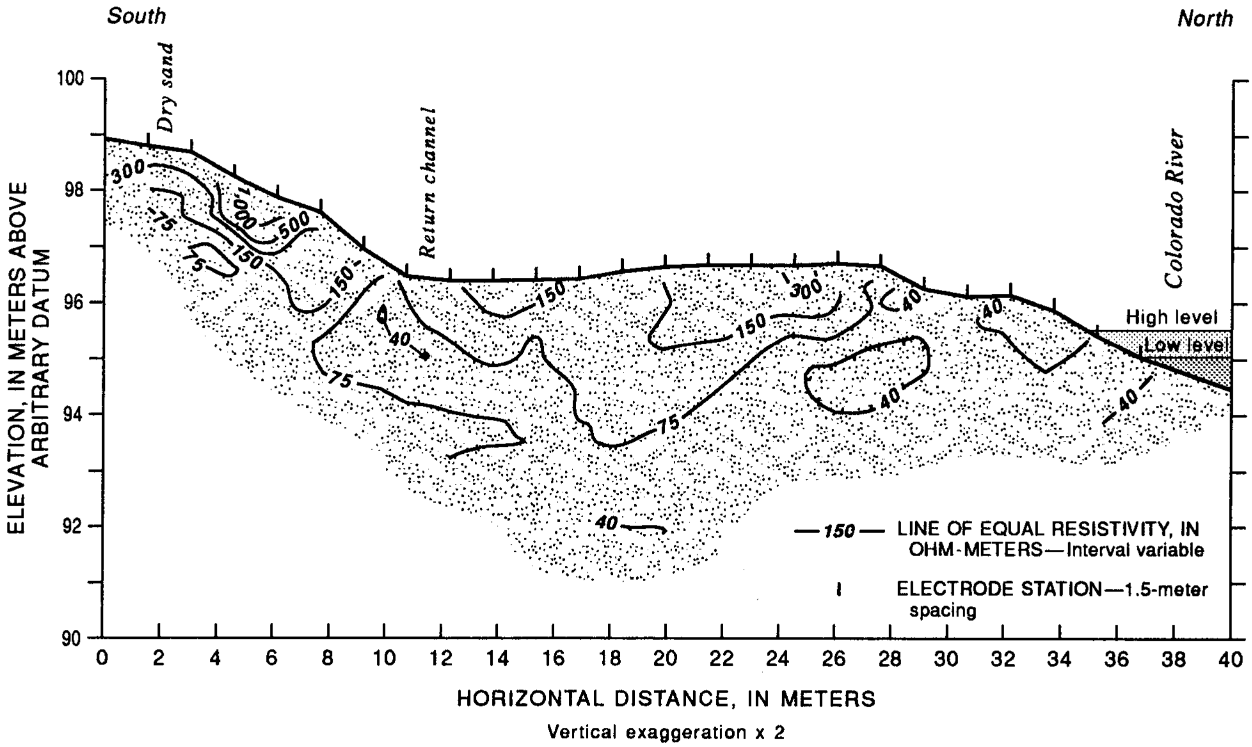

Figure 13. Modified logarithmic pseudosection of apparent resistivity referenced to land surface at sandbar 172.3L, downstream from the mouth of National Canyon, August 1991.

from the opposite bank, indicate that duration of drainage is an important factor in rill erosion. Reduced weekend flows cause enhanced rilling, and constant low flows (140 m^3/s) after high flows produce intense rilling until a sandbar is drained. In general, minimizing the rate and magnitude of downramping would minimize seepage erosion and consequent slumping and fissuring.

Observed rill erosion and slumping accompanied by measured tilts continued in reduced magnitude during interim flows on sandbar 43.1L after a reduction in the range of discharge from 85 to 800 m^3/s to a range of 340 to 570 m^3/s. This modification reduced stage fluctuation to less than 2 m. If a threshold value of stage fluctuation necessary for rilling exists, the threshold has been demonstrated to be less than the interim flow regime of 340 to 570 m^3/s. Quantitative estimates of stage fluctuations necessary for initiation of rilling will result from stress-strain and variably saturated flow analysis.

Ground-water processes occur on every sandbar and become increasingly important if sandbar-building flows do not occur or are widely spaced in time. Probably no set of prescribed sandbar-building flows will rebuild all sandbars. Thus, ground-water processes increase in importance on those sandbars that are not rebuilt.

SUMMARY AND CONCLUSIONS

Three sandbars along the Colorado River in Grand Canyon were instrumented with sensors for continual monitoring of stage, pore pressure, ground-water temperature, and tilt to determine the relation between ground-water flow and sandbar deformation. Typically, in a sandbar, five vertical clusters of deep, intermediate, and shallow pairs of pore-pressure and temperature sensors were installed in a vertical plane orthogonal to the river's edge.

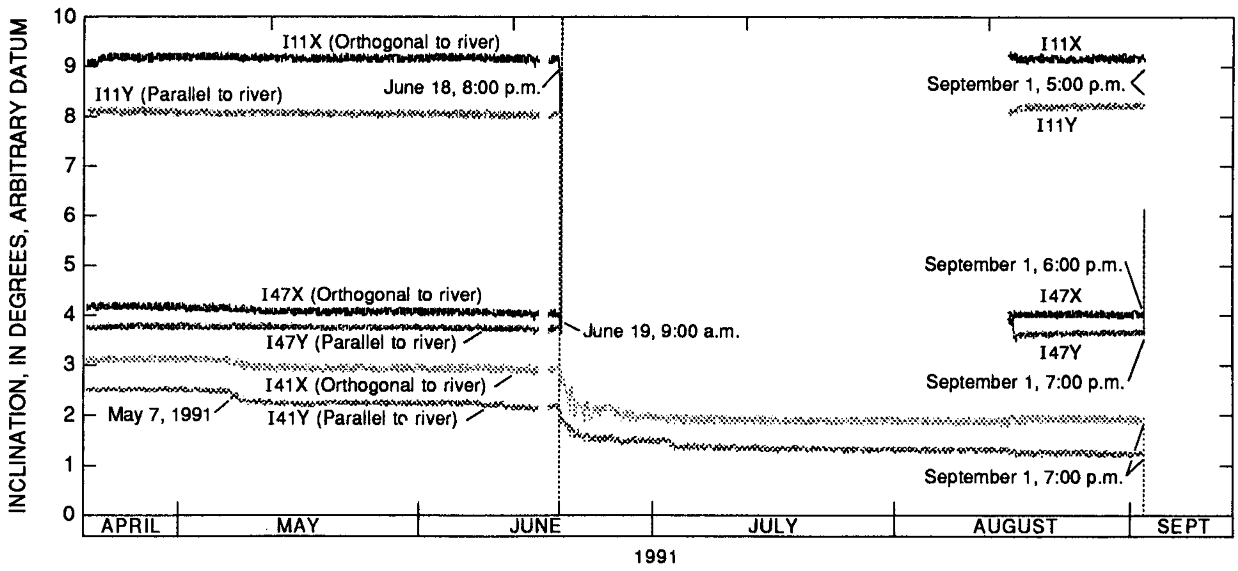

Figure 14. Tilt for sensor I18, I41, and I47 at sandbar 172.3L, downstream from the mouth of National Canyon, April 19 through September 12, 1991.

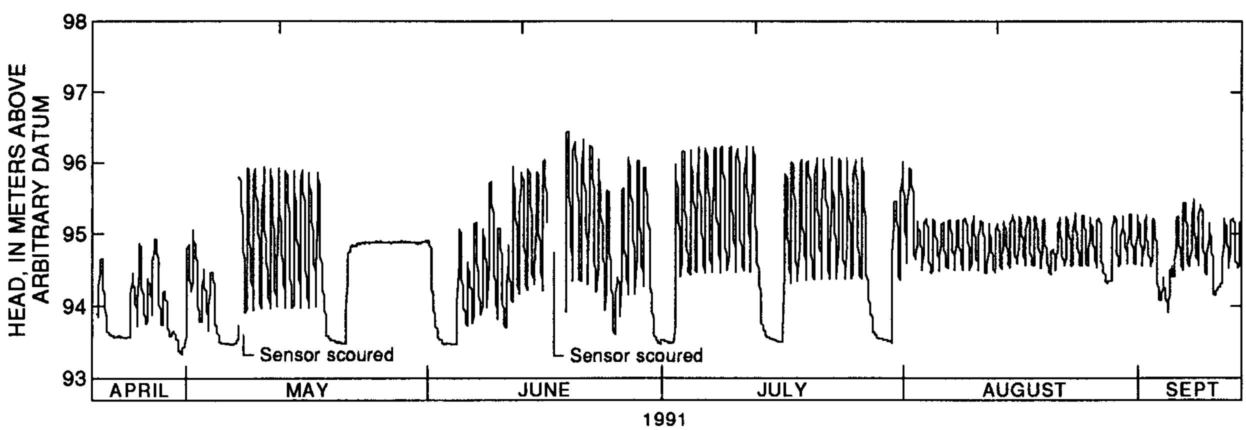

Figure 15. River stage at sandbar 172.3L, downstream from the mouth of National Canyon, April 19 through September 12, 1991.

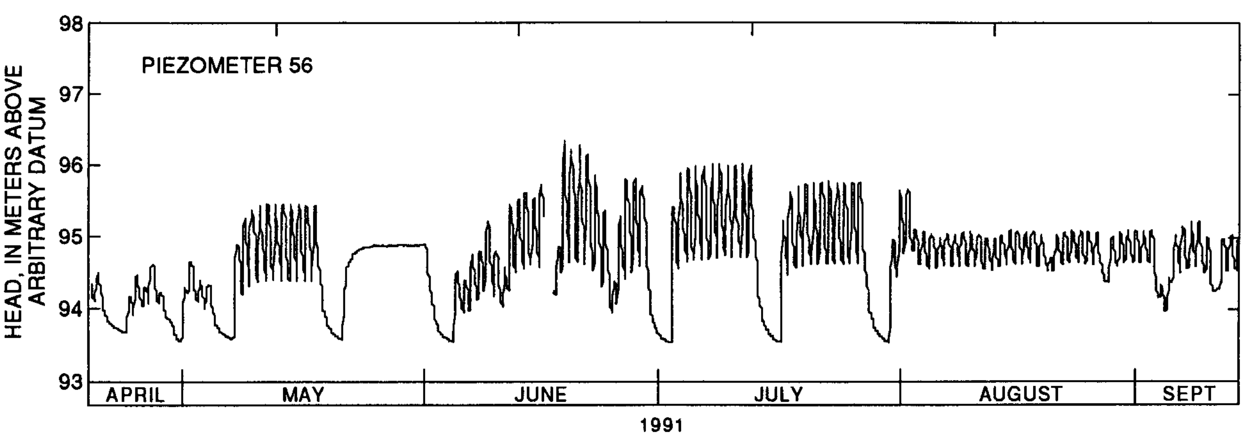

Figure 16. Water level in piezometer 56 at sandbar 172.3L, downstream from the mouth of National Canyon, April 19 through September 12, 1991.

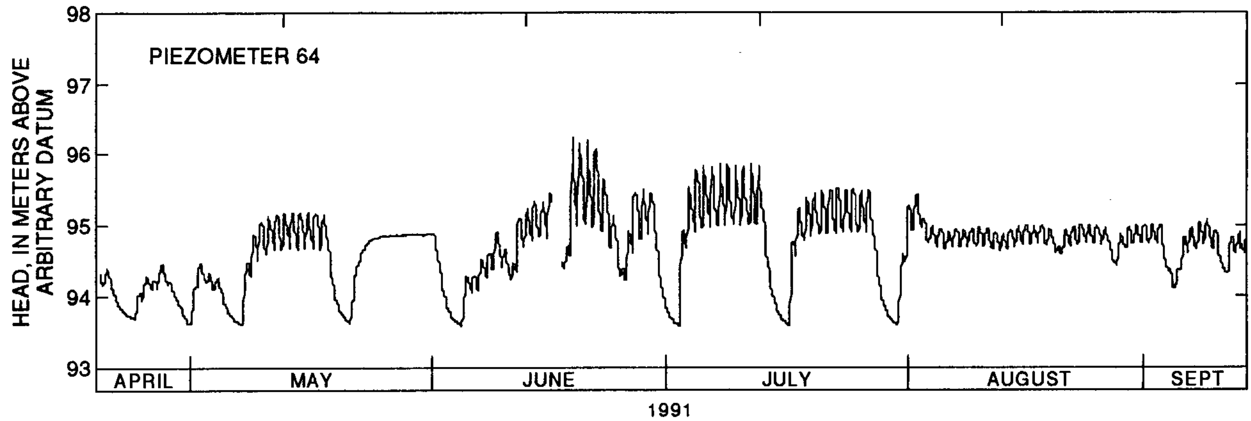

Figure 17. Water level in piezometer 64 at sandbar 172.3L, downstream from the mouth of National Canyon, April 19 through September 12, 1991.

The stratigraphies of the three sandbars varied considerably. At sandbar –6.5R, a unit of homogeneous fine to medium sand contained an interlayer or confining unit of silty, very fine sand. This unit dipped toward the back of the sandbar where it flattened and attained a depth of about 3.5 m. This sandbar had a gentle slope in the zone of fluctuating river stage and exhibited a seepage face with rill erosion but did not exhibit slumping and fissuring. At sandbar 43.1L, homogeneous, fine to medium sand overlay medium salt-and-pepper sand at a depth of 6 m. A lens of reddish, silty sand with some gravel occurred at a depth of about 4 m in the back of the sandbar. The zone of fluctuating river stage was a steeply sloping face that exhibited rill erosion, slumping, and fissuring. At sandbar 172.3L, fine to medium sand was interlayered with silty, very fine sand. The broad, shallow return channel was underlain with silty fine sand. The zone of fluctuating river stage was a steeply sloping face with a bench that was underlain with reddish, silty, very fine sand interlayered with fine to medium sand. This sandbar exhibited rill erosion, slumping, and fissuring.

Pole-pole DC resistivity was shown to produce useful results in a difficult environment. Sandbar 43.1L displayed a reasonably well-defined layered-earth response, whereas sandbar 172.3L displayed more lateral contrasts and only weakly defined layering. The contrast in geophysical character of the two sandbars may represent a difference in erosional-depositional environments between an upper pool deposit (43.1L) and a reattachment deposit (172.3L).

At sandbar 43.1L, tilts consistent with slumping and creep occurred from July 7 through July 26, 1991. All of the sudden tilts except one minor positive tilt occurred on downward limbs of hydrographs when the effective stress in the sandbar face was increasing. One hypothesis that explains these tilts is a slump-creep sequence of downslope movement in which tilt alternates from positive to negative. An alternative hypothesis is slumping or rotational failure with the tilt sensor within a slump block during the major positive event and outside a block on succeeding tilts. The probable cause of slope failure on this sandbar was oversteepening of the lower part of the slope of the zone of fluctuating river stage by rilling. This effect was increased by longer drainage times during fluctuating weekend low flows and steady low flows. Oversteepening of the lower part of the face of the zone of fluctuating river stage accumulated to a critical value. Then, slumping was triggered by a change in effective stress during the falling limb of the hydrograph. Attenuation of water-level fluctuation from the front to the back of sandbar 43.1L was 30 percent over a distance of 30 m.

At sandbar 172.3L, tilts probably were all related to scour. All tilts that were documented by tilt sensors occurred on the rising limb of a hydrograph. Tilts occurred on April 17, May 7, May 13, June 18, and September 1, 1991. Negative tilts toward the river occurred on May 7 and June 18. On September 1, the entire face of sandbar 172.3L was scoured and three tilt sensors went off scale. Attenuation of water-level fluctuation from the stage sensor to the back of the sandbar was about 65 percent over 35 m.

Seepage erosion, slumping, and fissuring mechanisms require a head gradient in the sandbar face toward the river; therefore, any steady-flow alternative would eliminate sandbar degradation resulting from these processes. Because duration of drainage and height of the seepage face are important in these processes, minimizing the rate and magnitude of downramping would minimize seepage erosion and consequent slumping and fissuring.

Observed rill erosion and slumping accompanied by measured tilts continued in reduced magnitude on sandbar 43.1L during interim flows. Thus, reduction in the range of discharge did not eliminate degradation caused by rill erosion, slumping, and fissuring. If there is a threshold range of stage fluctuation below which rilling did not occur, that range is less than the interim flow regime. The importance of the ground-water processes is that they occur on every sandbar. The processes become increasingly important on all sandbars in the absence of sandbar-building flows or if sandbar-building flows are widely spaced in time. Probably no set of prescribed sandbar-building flows will rebuild all sandbars. Thus, ground-water processes gain importance on sandbars that are not rebuilt.

SELECTED REFERENCES

Carpenter, M.C., Carruth, R.L., and Cluer, B.L., 1991, Beach erosion and deformation caused by outward flowing bank storage associated with fluctuating flows along the Colorado River in the Grand Canyon [abs.]: American Geophysical Union Transactions, v. 72, no. 44, p. 222.

Carpenter, M.C., Crosswhite, J.A., and Carruth, R.L., 1995, Water-level fluctuations, water temperatures, and tilts in sandbars –6.5R, 43.1L, and 172.3L, Grand Canyon, Arizona, 1990–93: U.S. Geological Survey Open-File Report 94–485, 17 p.

Carruth, R.L., Carpenter, M.C., and Cluer, B.L., 1991, Documentation of beach failure caused by slumping and seepage erosion at two sites on the Colorado River in the Grand Canyon [abs.]: American Geophysical Union Transactions, v. 72, no. 44, p. 223.

Cluer, B.L., 1991, Catastrophic erosion events and rapid deposition of sandbars on the Colorado River, the Grand Canyon, Arizona [abs.]: American Geophysical Union Transactions, v. 72, no. 44, p. 223.

Cluer, B.L., Carpenter, M.C., Martin, L.J., Wondzell, M.A., Dexter, L.R., and Manone, M.F., 1993, Rapid erosion and slow redeposition of sand bars along the regulated Colorado River in the Grand Canyon [abs.]: American Geophysical Union Transactions, v. 74, no. 43, p. 321.

Fink, J.B., 1989, Induced polarization: electrochemistry, fractal geometry, and geohydrologic applications: Tucson, University of Arizona, unpublished Ph.D. dissertation, 585 p.

Howard, A.D., and McLane, C.F., III, 1988, Erosion of cohesionless sediment by groundwater seepage: Water Resources Research, v. 24, no. 10, p. 1659–1674.

Iverson, R.M., and Major, J.J., 1986, Groundwater seepage vectors and the potential for hillslope failure and debris flow mobilization: Water Resources Research, v. 22, no. 11, p. 1543–1548.

Schmidt, J.C., and Graf, J.B., 1990, Aggradation and degradation of alluvial sand deposits, 1965 to 1986, Colorado River, Grand Canyon National Park, Arizona: U.S. Geological Survey Professional Paper 1493, 74 p.

Werrell, W.L., Inglis, R.R., and Martin, L.J., 1991, Beach face erosion in the Grand Canyon during falling stage of the Colorado River [abs.]: American Geophysical Union Transactions, v. 72, no. 44, p. 224.

GPO 684-855/39097